Theoretical scheme of thermal-light many-ghost imaging by Nth-order intensity correlation

Ying-Chuan Liu[1,2] and Le-Man Kuang[1,*]

[1]*Key Laboratory of Low-Dimensional Quantum Structures and Quantum Control of Ministry of Education, and Department of Physics, Hunan Normal University, Changsha 410081, China*

[2]*College of Mathematics and Physics, University of South China, Hengyang 421001, China*

(Received 28 March 2009; published 6 May 2011)

In this paper, we propose a theoretical scheme of many-ghost imaging in terms of Nth-order correlated thermal light. We obtain the Gaussian thin lens equations in the many-ghost imaging protocol. We show that it is possible to produce $N-1$ ghost images of an object at different places in a nonlocal fashion by means of a higher order correlated imaging process with an Nth-order correlated thermal source and correlation measurements. We investigate the visibility of the ghost images in the scheme and obtain the upper bounds of the visibility for the Nth-order correlated thermal-light ghost imaging. It is found that the visibility of the ghost images can be dramatically enhanced when the order of correlation becomes larger. It is pointed out that the many-ghost imaging phenomenon is an observable physical effect induced by higher order coherence or higher order correlations of optical fields.

DOI: 10.1103/PhysRevA.83.053808 PACS number(s): 42.50.Ar, 42.30.Va, 42.50.Dv

I. INTRODUCTION

Ghost imaging [1] is a technique to image nonlocally an object by the use of correlated light beams. Two types of ghost imaging have been experimentally demonstrated. Type-one ghost imaging [2,3] uses entangled photon pairs as the light source while type-two ghost imaging uses chaotic thermal light. In ghost imaging, the object and image are separately illuminated by a pair of correlated light beams, and the image emerges through coincidence detection of the two beams. As is well known, in classical imaging techniques based on geometrical optics, the image of an object can be produced by a lens in the plane defined by the Gaussian thin lens equation. The lens has the ability to generate a one-to-one relationship between points of the object and image planes. A perfect point-to-point image-forming relationship between the object and image planes produces a perfect image. All different momenta passing through a point of the object are collected by the lens into a point of the image plane. Differently from the classical imaging techniques, in ghost imaging, the light source consists of pairs of correlated photons emitted with all possible momenta and in all possible directions. If one photon is measured to have a certain transverse momentum, the transverse momentum of the other one is immediately known. A point-to-point relationship between the object and image planes arises by counting coincidences between the two distant detectors and leads to a ghost image of the object whenever a proper Gaussian thin lens equation is satisfied.

Ghost imaging with thermal light [4–24] has been studied extensively in recent years. Bennink and coworkers [4] first pointed out that ghost imaging can also be realized using a classical source with appropriate correlations. A thermal or quasithermal source can exhibit such classical correlations. A very close formal analogy was demonstrated between ghost imaging with thermal and quantum-entangled optical beams in Refs. [6–9], which showed that classically correlated optical beams were able to emulate the relevant features of quantum ghost imaging. A number of experiments on thermal-light ghost imaging have been performed in Refs. [12–15,24]. A unified treatment of classical and quantum ghost imaging was established in terms of Gaussian-state analysis in Ref. [16].

Recently, some attention has been paid to the physics of thermal-light ghost imaging [1,15,25–31] and higher-order-coherence or higher-order-correlation effects of thermal light [32–40]. The higher order coherence or higher order correlations have shown attractive properties in practical applications. Multiphoton imaging with thermal light is one of these exciting areas. In a previous work, our group theoretically initiated a study of thermal-light ghost imaging in terms of higher order correlated thermal light [32]. We proposed a thermal-light ghost imaging scheme with third-order correlated thermal light. In this scheme, a third-order correlated thermal-light source, a test optical arm, and two reference optical arms are used to produce two ghost images. Two ghost images are created at two different places in a nonlocal fashion as a consequence of the third-order correlation of the involved optical fields. It was shown that the third-order correlated imaging includes richer correlated imaging effects than the second-order correlated one. In Refs. [36,37], arbitrary Nth-order ($N \geqslant 2$) lensless ghost imaging with thermal light has been performed by only recording the intensities in two optical paths, and it is shown that the image visibility can be dramatically enhanced as the order N increases. In this paper, we want to propose a thermal-light many-ghost imaging scheme with Nth-order intensity correlations and N optical paths. Differently from the scheme in Refs. [36–38], our scheme can produce $N-1$ ghost images by the use of one test optical arm and $N-1$ reference optical arms. We investigate the visibility of the ghost images. We show that the usual second- and third-order ghost imagings with thermal light are only two particular examples of our present scheme.

The paper is organized as follows. In Sec. II, by the use of a thermal-light source with Nth-order correlation, we will propose the thermal-light many-ghost imaging scheme with Nth-order intensity correlation. In Sec. III, the visibility of

*Author to whom any correspondence should be addressed.

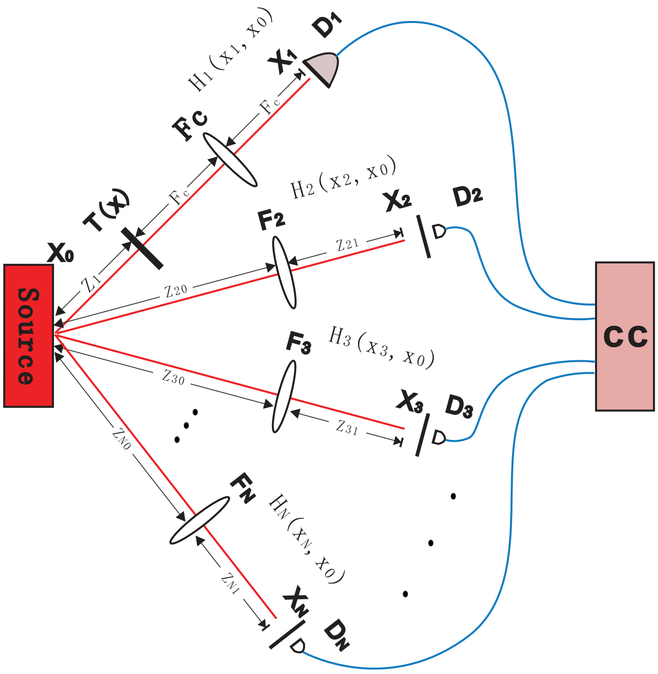

FIG. 1. (Color online) Schematic of the setup for implementing ghost imaging with Nth-order correlated thermal light. It consists of one test arm and $N-1$ reference arms. The test arm includes the imaged object with the transmission function $T(x)$, the collection lens F_c, and the bucket detector D_1. The object and the detector are placed in its two focal planes of the collection lens, respectively. Each reference arm includes one imaging lens and a scanning detector denoted by F_i and D_i with $i = 2,3,\ldots,N$, respectively.

the ghost images in the proposed scheme will be investigated. Finally, we shall conclude our paper with discussions and remarks in the last section.

II. MANY-GHOST IMAGING SCHEME

The basic setup for many-ghost imaging with N-order correlated thermal light is indicated in Fig. 1 which includes one test optical arm and $N-1$ reference optical arms. The first arm is the test arm. An unknown object with transmission function $T(x)$ and a collective lens with focal length f_c are placed on the test arm while there is one imaging lens with focal lengths f_i on each reference arm. The object is placed at the focal plane of the collective lens at distance z_1 from the thermal-light source. The distance between the ith imaging lens and the thermal-light source is z_{i0} with $i = 2,3,\ldots,N$. The first detector D_1 is a bucket detector placed at the focal plane of the collective lens on the right-hand side. The other detectors are scanning detectors D_i with $i = 2,3,\ldots,N$ which are placed at distances z_{i1} from ith imaging lens. The signals from the N photon counting detectors are sent to an electronic coincidence circuit to measure the rate of coincidence counts.

The thermal-light source with Nth-order intensity correlation, usually obtained by illuminating a laser beam into a slowly rotating ground glass, is divided into N beams, which can be implemented by an appropriate combination of $N-1$ beam splitters. Consider a monochromatic plane wave described by the field $E_0 \exp[i(k_0 z - w_0 t)]$ illuminating a material containing disordered scattering centers. After scattering, the field can be written as $E(x,z,t) = \int E(\mathbf{q}) \exp[i(\mathbf{q}\cdot\mathbf{x} + k_z z - w_0 t)] d\mathbf{q}$ where $\mathbf{q}$ is the transverse wave vector introduced by the random scattering and satisfies the relation $|\mathbf{q}|^2 + k_z^2 = k_0^2$. Hence, $E(\mathbf{q})$ is a stochastic variable obeying Gaussian statistics. However, the scattered waves with different transverse wave vectors are statistically independent. If $|\mathbf{q}| \ll k_0$, the scattered field can be approximately written as $E(x,z,t) = A(x)\exp[i(k_0 z - w_0 t)]$ where $A(x) = \int E(\mathbf{q}) \exp[i(\mathbf{q}\cdot\mathbf{x})] d\mathbf{q}$ is the slowly varying envelope. As a result, we have defined a monochromatic thermal light random in both strength and propagation direction. According to the Wiener-Khintchine theorem, the first-order spectral correlation satisfies the following expression:

$$\langle E^*(\mathbf{q})E(\mathbf{q}')\rangle = S(\mathbf{q})\delta(\mathbf{q}-\mathbf{q}'), \tag{1}$$

where $S(\mathbf{q})$ is the power spectrum of the spatial frequency. For any field with thermal statistics, all high-order correlations can be expressed in terms of the first-order ones due to $\langle E(\mathbf{q})\rangle = 0$ [41]. Then, Nth-order spectral correlation of thermal light can be written a

$$\left\langle \prod_{i=1}^{N} E^*(\mathbf{q}_i)E(\mathbf{q}_i')\right\rangle = \sum_{\substack{r_1,r_2,\ldots,r_N = 1, r_1\neq r_2\neq\cdots\neq r_N \\ s_1,s_2,\ldots,s_N = 1, s_1\neq s_2\neq\cdots\neq s_N}}{}' \left(\prod_{i=1}^{N}\delta(\mathbf{q}_{r_i}-\mathbf{q}_{s_i}')\right) S(\mathbf{q}_1)S(\mathbf{q}_2)\cdots S(\mathbf{q}_N), \tag{2}$$

where the prime in the summation means that all of the repeating terms are subtracted from the summation over r_i and s_i with both r_i and s_i taking $1,2,\ldots,N$ for $i = 1,2,\ldots,N$. In Eq. (2) $\mathbf{q}_{r_i}$ and $\mathbf{q}_{s_i}'$ are the transverse wave vector in r_ith optical arm. After passing through a combination of $N-1$ beam splitters, the thermal light with Nth-order spectral correlation is divided into N correlated thermal-light beams which are input light beams of the test and reference arms, respectively. For simplicity, we consider the one-dimensional case and let x_0 and x_n with $n = 1,2,\ldots,N$ be the transverse coordinates of the source plane and detection planes, respectively. Here we have assumed that the starting planes of the N thermal-light beams are overlapped. Let $H_1(x_1,x_0)$ be the impulse response function of the test arm and $H_n(x_n,x_0)$ with $n = 2,3,\ldots,N$ be the impulse response function of the nth reference arm, respectively. Assume that the light field on the nth detection plane is denoted as $E(x_n)$, which is connected with the optical field of the thermal-light source through the following relation:

$$E(x_n) = \int h_n(x_n, -q_n)\, E(q_n)\, dq_n, \tag{3}$$

where $h_n(x_n,q_n) = (1/\sqrt{2\pi})\int H_n(x_n,x_0)\exp(-iq_n x_0)dx_0$ is the Fourier transformation of the impulse response function

$H_n(x_n,x_0)$. Then, the Nth-order spatial correlation function of the joint intensity at the N detection planes can be expressed in terms of the Nth-order spectral correlation function and the impulse response functions as

$$\begin{aligned} G^{(N)}&(x_1,x_2,\ldots,x_N) \\ &= \langle E^*(x_1)E(x_1')E^*(x_2)E(x_2')\cdots E^*(x_N)E(x_N')\rangle \\ &= \int h_1^*(x_1,-q_1)h_1(x_1,-q_1')h_2^*(x_2,-q_2)h_2(x_2, \\ &\quad -q_2')\cdots h_N^*(x_N,-q_N)h_N(x_N,-q_N')\langle E^*(q_1)E(q_1') \\ &\quad \times E^*(q_2)E(q_2')\cdots E^*(q_N)F(q_N')\rangle \\ &\quad \times dq_1dq_1'dq_2dq_2'\cdots dq_Ndq_N'. \end{aligned} \tag{4}$$

The rate of coincidence counts is governed by the Nth-order spatial correlation function given by Eq. (4) which can be calculated in terms of the impulse response functions of the relevant optical systems. The impulse response functions [42] in the reference arms can be written as

$$h_r(x_r,q) = \sqrt{\frac{f_r}{2\pi(f_r - z_{r1})}}e^{i\varphi_r(x_r,q)}, \tag{5}$$

$$\begin{aligned} \varphi_r(x_r,q) = k(z_{r0}+z_{r1}) - \frac{q^2}{2k}\left(z_{r0} + \frac{z_{r1}f_r}{f_r - z_{r1}}\right) \\ - \frac{(2qf_r + kx_r)x_r}{2(f_r - z_{r1})}, \end{aligned} \tag{6}$$

where $z_{r1} \neq f_r$ with $r = 2,3,\ldots,N$, and the impulse response function in the test arm is given by

$$\begin{aligned} h_1(x_1,q) = \frac{1}{2\pi}\sqrt{\frac{k}{if_c}}\exp\left[ik(z_1+2f_c) + \left(-i\frac{z_1q^2}{2k}\right)\right] \\ \times \int T(x)\exp\left[-i\left(\frac{kx_1}{f_c}+q\right)x\right]dx, \end{aligned} \tag{7}$$

where $T(x)$ is the transmission function of the imaged object.

Substituting the Nth-order spectral correlation function given by Eq. (2) and the impulse response functions given by Eqs. (5) and (7) into Eq. (4), we can obtain the Nth-order spatial correlation function which can be expressed by the following two kinds of integrations:

$$I_n = \int S(q)|h_n(x_n,-q)|^2dq, \tag{8}$$

$$C_{nn'} = \int S(q)h_n^*(x_n,-q)h_{n'}(x_{n'},-q)dq, \tag{9}$$

where both n and n' may take $1,2,\ldots,N$, but $r \neq n'$. In the broadband limit, $S(q)$ can be regarded as a constant $S(0)$. Hence we have the total intensity of the thermal light $S_0 = \int S(q)dq \approx S(0)q_0$, where the spectral bandwidth of the source [43] is given by the parameter q_0, which depends on the wavelength of the thermal-light source, the diameter of the light beam, and the distance between the imaged object and the light source. Obviously, the case of $q_0 = 0$ is meaningless since the ghost image cannot be generated in this case. Substituting the impulse response functions of the test and reference arms given by Eqs. (5) and (7) into Eqs. (8) and (9), we obtain

$$\begin{aligned} I_1 &= \frac{S(0)k}{4\pi^2 f_c}\int|T(x)|^2dx, \\ I_r &= \frac{f_rS(0)q_0}{2\pi(f_r - z_{r1})}, \end{aligned} \tag{10}$$

$$C_{r1} = \frac{S(0)}{2\pi}\sqrt{\frac{kf_r}{i2\pi f_c(f_r - z_{r1})}}\int T(x)e^{i\phi_{r1}(x,q)}dx\,dq, \tag{11}$$

$$C_{rr'} = \frac{S(0)}{2\pi}\sqrt{\frac{f_rf_{r'}}{(f_r - z_{r1})(f_{r'} - z_{r'1})}}\int e^{i\phi_{rr'}(q)}dq, \tag{12}$$

where both r and r' may take $2,3,\ldots,N$ but $r \neq r'$, and we have introduced two phase functions

$$\begin{aligned} \phi_{r1}(x,q) = \frac{q^2}{2k}\left(z_{r0} - z_1 + \frac{z_{r1}f_r}{f_r - z_{r1}}\right) - \left(q + \frac{kx_1}{f_c}\right)x \\ + qX_r - k(z_{r0} + z_{r1} - z_1 - 2f_c), \end{aligned} \tag{13}$$

$$\begin{aligned} \phi_{rr'}(q) = \frac{kx_r^2}{2(f_r - z_{r1})} - \frac{kx_{r'}^2}{2(f_{r'} - z_{r'1})} \\ - \frac{q^2}{2k}\left(z_{r'0} - z_{r0} + \frac{z_{r'1}f_r'}{f_r' - z_{r'1}} - \frac{z_{r1}f_r}{f_r - z_{r1}}\right) \\ - q(X_{r'} - X_r) + k(z_{r'0} + z_{r'1} - z_{r0} - z_{r1}), \end{aligned} \tag{14}$$

where the scaled transverse positions are defined by

$$X_r = \frac{f_rx_r}{f_r - z_{r1}} \qquad (r = 2,3,\ldots,N). \tag{15}$$

From Eqs. (11)–(13), it is straightforward to see that when the positions of the object, ghost images, and the lenses obey the following Gaussian thin lens equations for the Nth-order correlated imaging,

$$\frac{1}{z_{r0} - z_1} + \frac{1}{z_{r1}} = \frac{1}{f_r} \qquad (r = 2,3,\ldots,N), \tag{16}$$

the cross-correlation functions of intensity fluctuation can be simplified as

$$\begin{aligned} C_{r1} = \frac{S(0)}{2\pi}\sqrt{\frac{kf_r}{i2\pi f_c(f_r - z_{r1})}}\exp\left(-\frac{ikx_1X_r}{f_c}\right)T(X_r) \\ \times\exp[-ik(z_{r_0} - z_{r_1} - z_1 - 2f_c)], \end{aligned} \tag{17}$$

$$C_{rr'} = \frac{S(0)}{2\pi}\sqrt{\frac{f_rf_{r'}}{(f_r - z_{r1})(f_{r'} - z_{r'1})}}e^{i\phi_{rr'}(0)}\delta(X_{r'} - X_r). \tag{18}$$

In the derivation of Eqs. (17) and (18) we have used the following properties of the δ function:

$$\begin{aligned} \frac{1}{2\pi}\int_{-\infty}^{\infty}e^{iqx}dq = \delta(x), \\ \int_a^b f(x)\delta(x - x_0)dx = f(x_0), \quad (a < x_0 < b). \end{aligned} \tag{19}$$

Equation (18) indicates that when $X_{r'} = X_r$ we have $C_{rr'} = \infty$ which means $G^{(N)}(x_1,x_2,\ldots,x_N) = \infty$. In this case, no ghost image can be observed since the visibility of the ghost imaging vanishes. This is different from the higher order lensless ghost imaging scheme with thermal light [36,37], in which working with equal values of X_r gives higher visibility.

When Gaussian thin lens equations are satisfied and $X_2 \neq X_3 \neq \cdots \neq X_N$, the Nth-order spatial correlation function of the joint intensity at the N detection planes given by Eq. (4) can be reduced to the following form:

$$G^{(N)}(x_1,x_2,\ldots,x_N) = \sum_{\substack{r_1,r_2,\ldots,r_{N-2}=2\\ r_1\neq r_2\neq\cdots\neq r_{N-2}}}^{N} (I_{r_1}I_{r_2}\cdots I_{r_{N-2}}|C_{r_{N-1}1}|^2)' + I_1I_2\cdots I_N, \tag{20}$$

where the prime on the right-hand side means that repeating terms in the summation over r_i and r_j $(i,j = 1,2,\ldots,N-2)$ should be subtracted. The last term on the right-hand equation (20) is the background term which is the multiplication of the intensity distribution at the N detectors. It does not contribute to the correlated imaging, but it may affect the visibility of produced ghost images. Each term in the summation over r_i and r_j is the multiplication of the intensity distribution at detector D_i and the intensity fluctuation correlation between D_1 and D_i with $i = 2,3,\ldots,N$, which gives the information of the object imaged at the detector D_i.

In particular, when the $N-1$ reference arms are identical, i.e., $f_2 = f_3 = \cdots = f_N$, $z_{20} = z_{30} = \cdots = z_{N0}$, and $z_{21} = z_{31} = \cdots = z_{N1}$, we have $I_2 = I_3 = \cdots = I_N \equiv I$, and the Nth-order correlation function becomes the following simple form:

$$G^{(N)} = I^{N-1}I_1 + \chi I^{N-2}\sum_{i=2}^{N}|T(X_i)|^2, \tag{21}$$

where we have introduced the parameter $\chi = S^2(0)kf_r/[8\pi^3 f_c(f_r - z_{r1})]$. Equation (21) indicates that for the object placed at the test arm, $N-1$ ghost images can be produced in the $N-1$ reference arms through coincidence count measurements upon N detectors. The Nth-order correlation function (21) gives one ghost image for each reference arm only when N coincidences are counted between the bucket detector, $N-2$ fixed pointlike detectors, and one scanning detector. Each ghost image is a magnified image of the object with the magnification factor $f_r/(f_r - z_{r1})$ with $r = 2,3,\ldots,N$ since $X_r = f_r x_r/(f_r - z_{r1})$. However, it should be pointed out that if the ghost image in any one of the $N-1$ reference arms is virtual, no Nth-order ghost image can be obtained since no N coincidences can be counted between the bucket detector, $N-2$ fixed pointlike detectors, and 1 scanning detector.

From the Gaussian thin lens equations of Nth-order correlated imaging given by Eq. (16) we can see that the higher order correlated imaging exhibits richer imaging effects. In fact, the imaging equation (16) indicates that $z_{r0} - z_1$ is the object distance while z_{r1} is the image distance for the rth joint path with $r = 2,3,\ldots,N$. Just as in the ordinary imaging law, when the object distance of the rth joint path $z_{r0} - z_1$ is greater (less) than the focal length f_r, the correlated image is real (virtual). As a specific example, we consider the case of $N = 4$. In this case, from the imaging equation (16) we can obtain the following eight ghost-image configurations: (1) when $z_{r0} - z_1 > f_r$ with $r = 2,3$, and 4, the three ghost images are real; (2) when $z_{r0} - z_1 < f_r$ with $r = 2,3$, and 4, the three ghost images are virtual; (3) when $z_{20} - z_1 > f_2$, $z_{30} - z_1 < f_3$, and $z_{40} - z_1 < f_4$, one ghost image is real at the position x_2 and the other two ghost images are virtual at the positions x_3 and x_4; (4) when $z_{30} - z_1 > f_3$, $z_{20} - z_1 < f_2$, and $z_{40} - z_1 < f_4$, the ghost image at the position x_3 and two ghost images at the positions x_2 and x_4 are virtual; (5) when $z_{40} - z_1 > f_4$, $z_{20} - z_1 < f_2$, and $z_{30} - z_1 < f_3$, the ghost image at the position x_4 is real and two ghost images at the positions x_2 and x_3 are virtual; (6) when $z_{20} - z_1 > f_2$, $z_{30} - z_1 < f_3$, and $z_{40} - z_1 < f_4$, two ghost images at the positions x_2 and x_3 are real and the ghost image at the position x_4 is virtual; (7) when $z_{20} - z_1 > f_2$, $z_{40} - z_1 < f_4$, and $z_{30} - z_1 < f_3$, two ghost images at the positions x_2 and x_4 are real and the ghost image at the position x_3 is virtual; (8) when $z_{30} - z_1 > f_3$, $z_{40} - z_1 < f_4$, and $z_{20} - z_1 < f_2$, two ghost images at the positions x_3 and x_4 are real and the ghost image at the position x_2 is virtual.

It is obvious that when $N = 2,3$, the usual results of the second- and third-order thermal-light ghost imaging [32] are recovered, respectively.

It should be pointed out that the physical mechanism of generating Nth-order correlation in our scheme is different that in Refs. [34,35]. In our scheme, Nth-order correlation is obtained by using coincidence measurements of N independent detectors which are located at the N optical arms with $N-1$ reference arms and one test arm. In the scheme in Refs. [34,35], Nth-order correlation is obtained by using only two CCD detectors which are located at two optical arms, one test arm and one reference arm. Nth-order intensity correlation is produced by the use of the intensity parting method in which the Nth-order correlation is composed of an n-fold intensity product at position x_1 and an $(N-n)$-fold intensity product at position x_2. Nth-order correlation can be measured by two CCD detectors located at positions x_1 and x_2. Then, in the Nth-order lensless ghost imaging there are at least $N-1$ experimental configurations since n may be different. In Refs. [34,35], the intensity values at different positions registered by the two CCDs are processed in a computer system to evaluate the higher order correlation. The total intensity of each frame recorded by the bucket detector CCD_1 at position x_1 in the test arm is divided by $N-1$ and convoluted with the output of CCD_2 which is captured at the same time at position x_2 in the reference arm. Hence, there are $(N-1)$-fold intensity products at position x_1 in the test arm and 1-fold intensity at position x_2 in the reference arm due to $n = N-1$. Equivalently, this implies that there are $N-1$ same test arms and only one reference arm. Therefore, only one ghost image can be produced in the reference arm.

It is interesting to note that our present scheme can become a lensless many-ghost imaging scheme by removing the imaging lenses F_i in Fig. 1. The lens F_c is a collecting lens; it can also be removed. From Eq. (16) we can see that the imaging equation becomes $Z_{r0} + Z_{r1} = Z_1$ in the absence of these imaging lenses; i.e., let $f_r \to \infty$ in Eq. (16). This indicates that we can obtain $N-1$ ghost images in the $N-1$ reference arms, and the distance between the rth ghost image and the light source in the rth reference arm is equal to that between the imaged object and the light source. In this case, making use of Eq. (15) we have $X_i = x_i$. Then from Eq. (21) we can see that the $N-1$ ghost image is identical to the imaged object. So the ghost images produced in the lensless many-ghost imaging cannot be magnified. If we use only two optical arms, one test arm and one reference arm, and adopt the intensity parting method in the test arm to produce an $(N-1)$-fold intensity product in the test arm, then we recover the lensless scheme in Refs. [34,35].

III. VISIBILITY OF GHOST IMAGES

The visibility is an important parameter for estimating the quality of a ghost image. We first generalize the visibility of the second-order correlated imaging [17,44] to the case of Nth-order correlated imaging as follows:

$$V^{(N)} = \frac{\left[G^{(N)} - \prod_{i=1}^{N}\langle I_i\rangle\right]_{\max}}{\left[G^{(N)}\right]_{\max}}. \tag{22}$$

For our present scheme of the Nth-order thermal-light imaging, substituting Eq. (21) into Eq. (22), we obtain the visibility

$$V^{(N)} = \frac{\left[\sum_{i=2}^{N}|T(X_i)|^2\right]_{\max}}{\left[q_0\int|T(x)|^2dx + \sum_{i=2}^{N}|T(X_i)|^2\right]_{\max}}, \tag{23}$$

which indicates that the visibility depends on not only the spectral bandwidth of the thermal-light source q_0 and the transmission function of the imaged object $T(x)$ but also the order number of the correlation of the thermal-light source. The visibility can be enhanced with the decrease of the spectral bandwidth. An increase of the transmission leads to a decrease of the visibility since when the transmission area increases, more points contribute to the background that directly makes the visibility decrease. It should be mentioned that the expression of the visibility (23) is obtained in the broadband limit which means $q_0 \gg 0$; therefore, the visibility is always less than the unit.

In order to see the relationship between the visibility and the order number of the correlation, making use of Eqs. (10) and (11), we have

$$\frac{\langle I_1\rangle\langle I_r\rangle}{|\langle E^*(x_1)E(x_r)\rangle|^2} = q_0\int|T(x)|^2dx, \tag{24}$$

where $r = 2,3,\ldots,N$. According to the Cauchy-Schwartz inequality $\langle I_1\rangle\langle I_r\rangle \geqslant |\langle E^*(x_1)E(x_r)\rangle|^2$, which means that $q_0\int|T(x)|^2dx \geqslant 1$. Hence, we find that

$$V^{(N)} \leqslant \frac{\left[\sum_{i=2}^{N}|T(X_i)|^2\right]_{\max}}{\left[1+\sum_{i=2}^{N}|T(X_i)|^2\right]_{\max}} \leqslant \frac{N-1}{N}, \tag{25}$$

which implies that the visibility of the ghost images can be dramatically enhanced when the order of correlation becomes larger. For Nth-order correlated thermal-light imaging, the upper bound of the visibility is given by $V_b^{(N)} = (N-1)/N$. As expected, when $N=2$ the upper bound of the visibility of the second correlated imaging [17] is 1/2.

To be specific, as an example we take the imaged object as a double slit with slit width of 0.1 mm and slit-slit spacing of 2.0 mm. The distance from the double slit to the thermal-light source is $Z1 = 50$ cm, and the wavelength of the pseudothermal source is $\lambda = 632.8$ nm. In this case, the visibility of the Nth-order correlated thermal-light ghost imaging is given by the expression $V_b^{(N)} = (N-1)/(2.97+N)$. In Fig. 2, the visibility of the ghost images for the double slit is plotted as a function the order N.

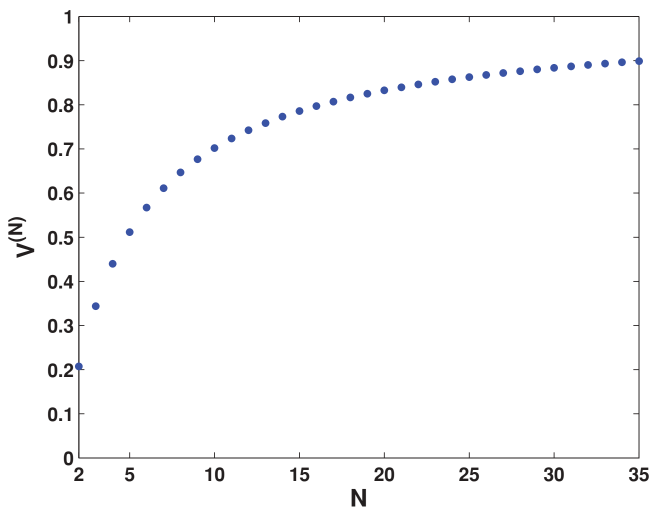

FIG. 2. (Color online) Curve of the visibility with respect to the order N in the Nth-order correlated thermal-light ghost imaging. Here we take the object as a double slit with slit width of 0.1 mm and spacing of 2.0 mm. The distance from the double slit to the light source is $Z1 = 50$ cm, and the wavelength of the pseudothermal source is $\lambda = 632.8$ nm.

It should be mentioned that the visibility of the correlated imaging is scheme dependent. The visibility of the correlated imaging in our scheme is slightly different from that in Ref. [36]. This is because the Nth-order correlated thermal-light ghost imaging scheme proposed in the present paper is different from the scheme in Ref. [36]. The former is a many-ghost imaging scheme which includes one test optical arm and $N-1$ reference optical arms; the latter is a single-ghost imaging scheme which incudes one test optical arm and only one reference optical arm. Besides, the former contains a lens while the latter essentially is an Nth-order lensless correlated ghost imaging scheme which is similar to the ones using second-order correlations in pseudothermal light [6,7].

IV. CONCLUDING REMARKS

In conclusion, we have proposed a theoretical scheme of ghost imaging in terms of Nth-order correlated thermal light. Our scheme includes one test arm and $N-1$ reference arms. The imaged object is placed on the test arm. $N-1$ ghost images are produced in the reference arms in a nonlocal fashion by means of a higher order correlated imaging process with an Nth-order correlated thermal source and correlation measurements. We have derived the Gaussian thin lens equations which the positions of the ghost images obey in the ghost imaging protocol. We have also investigated the visibility of the ghost images in the scheme and obtained the upper bounds of the visibility for the Nth-order correlated thermal-light ghost imaging. It has been shown that the visibility depends on not only the spectral bandwidth of the thermal-light source and the transmission area of the object but also the order number of the correlation of the thermal-light source. It is found that the visibility of the ghost images can be dramatically enhanced when the order of correlation becomes larger. The present many-ghost imaging protocol could have promising applications. On one hand, it gives rise to a theoretical origin for developing many-ghost imaging technology. This gives rise to the possibility of experimentally producing correlated many-ghost images. In fact, the higher order correlated imaging opens up new avenues for realizing multiport information processing. On the other hand, physically these ghost images stem from higher order coherence or higher order correlations of optical fields. In this sense, the appearance of the many-ghost images reveals an observable physical effect of higher order coherence or higher order correlations of optical fields. Hence, it is of very significance to study higher order correlated imaging not only for understanding well the essential physics behind the higher coherence or higher order correlations of optical fields but also for developing multiport information processing technology. The experimental realization for the many-ghost imaging protocol proposed here and practical applications of the many-ghost imaging phenomenon deserves further investigation.

ACKNOWLEDGMENTS

We would like to thank the referee for his or her helpful and stimulating comments. This work was supported by National Fundamental Research Program Grant No. 2007CB925204, the National Natural Science Foundation under Grants No. 10775048 and No. 11075050, the Program for Changjiang Scholars and Innovative Research Team in University under Grant No. IRT0964, and Research Fund of Hunan Provincial Education Department Grant No. 08W012.

APPENDIX: DERIVATION OF NTH-ORDER SPECTRAL CORRELATION FUNCTION OF THERMAL LIGHT

In this appendix, we wish to present the derivation of the Nth-order spectral correlation function of thermal light given by Eq. (2). The Nth-order spectral correlation of thermal light is given by

$$\left\langle \prod_{i=1}^{N} E^*(\mathbf{q}_i)E(\mathbf{q}_i') \right\rangle = \langle E^*(q_1)E(q_1')E^*(q_2)E \times (q_2') \cdots E^*(q_N)E(q_N')\rangle. \tag{A1}$$

According to the moment theorem for a Gaussian random process, the Nth-order spectral correlation of thermal light can be expanded in terms of the first-order field correlations as

$$\left\langle \prod_{i=1}^{N} E^*(\mathbf{q}_i)E(\mathbf{q}_i') \right\rangle = \sum_{N!} C_{11}(q_1,q_1')C_{22} \times (q_2,q_2') \cdots C_{NN}(q_N,q_N'), \tag{A2}$$

where $\sum_{N!}$ denotes summation over all the $N!$ possible permutations of the variables $\{q_1',q_2',\ldots,q_N'\}$, and the correlation functions $C_{ij}(q_i,q_j')$ are defined by

$$C_{ij}(q_i,q_j') = \langle E^*(q_i)E(q_j)\rangle. \tag{A3}$$

For thermal light with Gaussian statistics, making use of Eq. (1) we have

$$C_{ij}(q_i,q_j') = S(q_i)\delta(q_i - q_j'). \tag{A4}$$

Substituting Eq. (A4) into (A2), we find that

$$\left\langle \prod_{i=1}^{N} E^*(\mathbf{q}_i)E(\mathbf{q}_i') \right\rangle = S(q_1)S(q_2)\cdots S(q_N) \times \sum_{N!} \delta(q_1 - q_1')\delta(q_2 - q_2') \times \cdots \delta(q_N - q_N'), \tag{A5}$$

where $\sum_{N!}$ also denotes summation over all the $N!$ possible permutations of the variables $\{q_1',q_2',\ldots,q_N'\}$.

In order to see the detailed structure of the Nth-order spectral correlation of thermal light given by Eq. (A5), we take the case of $N = 4$ as an example. In this case, the fourth-order spectral correlation given by Eq. (A5) $\langle \prod_{i=1}^{4} E^*(\mathbf{q}_i)E(\mathbf{q}_i')\rangle$ can be explicitly expressed as

$$\begin{aligned}
&S(\mathbf{q}_1)S(\mathbf{q}_2)S(\mathbf{q}_3)S(\mathbf{q}_4)\\
&\times \{\delta(\mathbf{q}_1 - \mathbf{q}_1')\delta(\mathbf{q}_2 - \mathbf{q}_2')\delta(\mathbf{q}_3 - \mathbf{q}_3')\delta(\mathbf{q}_4 - \mathbf{q}_4')\\
&+ \delta(\mathbf{q}_1 - \mathbf{q}_1')\delta(\mathbf{q}_2 - \mathbf{q}_2')\delta(\mathbf{q}_3 - \mathbf{q}_4')\delta(\mathbf{q}_4 - \mathbf{q}_3')\\
&+ \delta(\mathbf{q}_1 - \mathbf{q}_1')\delta(\mathbf{q}_2 - \mathbf{q}_3')\delta(\mathbf{q}_3 - \mathbf{q}_2')\delta(\mathbf{q}_4 - \mathbf{q}_4')\\
&+ \delta(\mathbf{q}_1 - \mathbf{q}_1')\delta(\mathbf{q}_2 - \mathbf{q}_3')\delta(\mathbf{q}_3 - \mathbf{q}_4')\delta(\mathbf{q}_4 - \mathbf{q}_2')\\
&+ \delta(\mathbf{q}_1 - \mathbf{q}_1')\delta(\mathbf{q}_2 - \mathbf{q}_4')\delta(\mathbf{q}_3 - \mathbf{q}_2')\delta(\mathbf{q}_4 - \mathbf{q}_3')\\
&+ \delta(\mathbf{q}_1 - \mathbf{q}_1')\delta(\mathbf{q}_2 - \mathbf{q}_4')\delta(\mathbf{q}_3 - \mathbf{q}_3')\delta(\mathbf{q}_4 - \mathbf{q}_2')\\
&+ \delta(\mathbf{q}_1 - \mathbf{q}_2')\delta(\mathbf{q}_2 - \mathbf{q}_1')\delta(\mathbf{q}_3 - \mathbf{q}_3')\delta(\mathbf{q}_4 - \mathbf{q}_4')\\
&+ \delta(\mathbf{q}_1 - \mathbf{q}_2')\delta(\mathbf{q}_2 - \mathbf{q}_1')\delta(\mathbf{q}_3 - \mathbf{q}_4')\delta(\mathbf{q}_4 - \mathbf{q}_3')\\
&+ \delta(\mathbf{q}_1 - \mathbf{q}_2')\delta(\mathbf{q}_2 - \mathbf{q}_3'\delta(\mathbf{q}_3 - \mathbf{q}_1')\delta(\mathbf{q}_4 - \mathbf{q}_4')\\
&+ \delta(\mathbf{q}_1 - \mathbf{q}_2')\delta(\mathbf{q}_2 - \mathbf{q}_3')\delta(\mathbf{q}_3 - \mathbf{q}_4')\delta(\mathbf{q}_4 - \mathbf{q}_1')\\
&+ \delta(\mathbf{q}_1 - \mathbf{q}_2')\delta(\mathbf{q}_2 - \mathbf{q}_4')\delta(\mathbf{q}_3 - \mathbf{q}_1')\delta(\mathbf{q}_4 - \mathbf{q}_3')\\
&+ \delta(\mathbf{q}_1 - \mathbf{q}_2')\delta(\mathbf{q}_2 - \mathbf{q}_4')\delta(\mathbf{q}_3 - \mathbf{q}_3')\delta(\mathbf{q}_4 - \mathbf{q}_1')\\
&+ \delta(\mathbf{q}_1 - \mathbf{q}_3')\delta(\mathbf{q}_2 - \mathbf{q}_1')\delta(\mathbf{q}_3 - \mathbf{q}_2')\delta(\mathbf{q}_4 - \mathbf{q}_4')\\
&+ \delta(\mathbf{q}_1 - \mathbf{q}_3')\delta(\mathbf{q}_2 - \mathbf{q}_1')\delta(\mathbf{q}_3 - \mathbf{q}_4')\delta(\mathbf{q}_4 - \mathbf{q}_2')\\
&+ \delta(\mathbf{q}_1 - \mathbf{q}_3')\delta(\mathbf{q}_2 - \mathbf{q}_2')\delta(\mathbf{q}_3 - \mathbf{q}_1')\delta(\mathbf{q}_4 - \mathbf{q}_4')\\
&+ \delta(\mathbf{q}_1 - \mathbf{q}_3')\delta(\mathbf{q}_2 - \mathbf{q}_2')\delta(\mathbf{q}_3 - \mathbf{q}_4')\delta(\mathbf{q}_4 - \mathbf{q}_1')\\
&+ \delta(\mathbf{q}_1 - \mathbf{q}_3')\delta(\mathbf{q}_2 - \mathbf{q}_4')\delta(\mathbf{q}_3 - \mathbf{q}_1')\delta(\mathbf{q}_4 - \mathbf{q}_2')\\
&+ \delta(\mathbf{q}_1 - \mathbf{q}_3')\delta(\mathbf{q}_2 - \mathbf{q}_4')\delta(\mathbf{q}_3 - \mathbf{q}_2')\delta(\mathbf{q}_4 - \mathbf{q}_1')\\
&+ \delta(\mathbf{q}_1 - \mathbf{q}_4')\delta(\mathbf{q}_2 - \mathbf{q}_1')\delta(\mathbf{q}_3 - \mathbf{q}_2')\delta(\mathbf{q}_4 - \mathbf{q}_3')\\
&+ \delta(\mathbf{q}_1 - \mathbf{q}_4')\delta(\mathbf{q}_2 - \mathbf{q}_1')\delta(\mathbf{q}_3 - \mathbf{q}_3')\delta(\mathbf{q}_4 - \mathbf{q}_2')\\
&+ \delta(\mathbf{q}_1 - \mathbf{q}_4')\delta(\mathbf{q}_2 - \mathbf{q}_2')\delta(\mathbf{q}_3 - \mathbf{q}_1')\delta(\mathbf{q}_4 - \mathbf{q}_3')\\
&+ \delta(\mathbf{q}_1 - \mathbf{q}_4')\delta(\mathbf{q}_2 - \mathbf{q}_2')\delta(\mathbf{q}_3 - \mathbf{q}_3')\delta(\mathbf{q}_4 - \mathbf{q}_1')\\
&+ \delta(\mathbf{q}_1 - \mathbf{q}_4')\delta(\mathbf{q}_2 - \mathbf{q}_3')\delta(\mathbf{q}_3 - \mathbf{q}_1')\delta(\mathbf{q}_4 - \mathbf{q}_2')\\
&+ \delta(\mathbf{q}_1 - \mathbf{q}_4')\delta(\mathbf{q}_2 - \mathbf{q}_3')\delta(\mathbf{q}_3 - \mathbf{q}_2')\delta(\mathbf{q}_4 - \mathbf{q}_1')\}.
\end{aligned} \tag{A6}$$

It is straightforward to see that the fourth-order spectral correlation given by Eq. (A6) can be rewritten as the following expression:

$$\left\langle \prod_{i=1}^{4} E^*(\mathbf{q}_i)E(\mathbf{q}'_i) \right\rangle = \sum_{r_i \neq r_j, s_i \neq s_j}^{4} \left(\prod_{i=1}^{4} \delta(\mathbf{q}_{r_i} - \mathbf{q}'_{s_i}) \right)' \times S(\mathbf{q}_1)S(\mathbf{q}_2)S(\mathbf{q}_3)S(\mathbf{q}_4), \quad \text{(A7)}$$

where the prime in the summation means that all of the repeating terms are subtracted from the summation over r_i and s_i with both r_i and s_i taking 1,2,3,4 for $i = 1,2,3,4$. It can be checked that for arbitrary N, the Nth-order spectral correlation of thermal light can be expressed as

$$\left\langle \prod_{i=1}^{N} E^*(\mathbf{q}_i)E(\mathbf{q}'_i) \right\rangle = \sum_{r_i \neq r_j, s_i \neq s_j}^{N} \left(\prod_{i=1}^{N} \delta(\mathbf{q}_{r_i} - \mathbf{q}'_{s_i}) \right)' \times S(\mathbf{q}_1)S(\mathbf{q}_2)\cdots S(\mathbf{q}_N), \quad \text{(A8)}$$

where the prime in the summation means that all of the repeating terms are subtracted from the summation over r_i and s_i with both r_i and s_i taking $1,2,\ldots,N$ for $i = 1,2,\ldots,N$. Equation (A8) is Eq. (2).

[1] Y. H. Shih, e-print arXiv:0805.1166v5 and references therein.
[2] T. B. Pittman, Y. H. Shih, D. V. Strekalov, and A. V. Sergienko, Phys. Rev. A **52**, 3429(R) (1995).
[3] D. N. Klyshko, Usp. Fiz. Nauk **154**, 133 (1988) [Sov. Phys. Usp. **31**, 74 (1988)]; D. N. Klyshko, Phys. Lett. A **132**, 299 (1988).
[4] R. S. Bennink, S. J. Bentley, and R. W. Boyd, Phys. Rev. Lett. **89**, 113601 (2002).
[5] A. Gatti, E. Brambilla, and L. A. Lugiato, Phys. Rev. Lett. **90**, 133603 (2003).
[6] A. Gatti, E. Brambilla, M. Bache, and L. A. Lugiato, Phys. Rev. Lett. **93**, 093602 (2004).
[7] A. Gatti, E. Brambilla, M. Bache, and L. A. Lugiato, Phys. Rev. A **70**, 013802 (2004).
[8] J. Cheng and S. S. Han, Phys. Rev. Lett. **92**, 093903 (2004).
[9] Y. Cai and S. Y. Zhu, Opt. Lett. **29**, 2716 (2004).
[10] Kam Wai Clifford Chan, M. N. O'Sullivan, and R. W. Boyd, Phys. Rev. A **79**, 033808 (2009).
[11] E. Brambilla, A. Gatti, M. Bache, and L. A. Lugiato, Fortschr. Phys. **52**, 1080 (2004).
[12] A. Valencia, G. Scarcelli, M. D'Angelo, and Y. H. Shih, Phys. Rev. Lett. **94**, 063601 (2005).
[13] F. Ferri, D. Magatti, A. Gatti, M. Bache, E. Brambilla, and L. A. Lugiato, Phys. Rev. Lett. **94**, 183602 (2005).
[14] D. Zhang, Y. H. Zhai, L. A. Wu, and X. H. Chen, Opt. Lett. **30**, 2354 (2005).
[15] R. Meyers, K. S. Deacon, and Y. Shih, Phys. Rev. A **77**, 041801(R) (2008).
[16] B. I. Erkmen and J. H. Shapiro, Phys. Rev. A **77**, 043809 (2008); **79**, 023833 (2009).
[17] A. Gatti, M. Bache, D. Magatti, E. Brambilla, F. Ferri, and L. A. Lugiato, J. Mod. Opt. **53**, 739 (2006).
[18] M. Bache, D. Magatti, F. Ferri, A. Gatti, E. Brambilla, and L. A. Lugiato, Phys. Rev. A **73**, 053802 (2006).
[19] Y. Cai and S. Y. Zhu, Phys. Rev. E **71**, 056607 (2005).
[20] Y. H. Zhai, X. H. Chen, D. Zhang, and L. A. Wu, Phys. Rev. A **72**, 043805 (2005).
[21] G. Scarcelli, V. Berardi, and Y. H. Shih, Phys. Rev. Lett. **96**, 063602 (2006).
[22] M. D'Angelo, Y. H. Kim, S. P. Kulik, and Y. H. Shih, Phys. Rev. Lett. **92**, 233601 (2004).
[23] H. Liu, X. Shen, D. M. Zhu, and S. Han, Phys. Rev. A **76**, 053808 (2007).
[24] M. Zhang, Q. Wei, X. Shen, Y. Liu, H. Liu, J. Cheng, and S. Han, Phys. Rev. A **75**, 021803(R) (2007).
[25] G. Scarcelli, V. Berardi, and Y. H. Shih, Appl. Phys. Lett. **88**, 061106 (2006).
[26] B. I. Erkmen and J. H. Shapiro, Phys. Rev. A **78**, 023835 (2008).
[27] A. Gatti, M. Bondani, L. A. Lugiato, M. G. A. Paris, and C. Fabre, Phys. Rev. Lett. **98**, 039301 (2007).
[28] L. G. Wang, S. Qamar, S. Y. Zhu, and M. S. Zubairy, Phys. Rev. A **79**, 033835 (2009).
[29] M. E. Brezinski and B. Liu, Phys. Rev. A **78**, 063824 (2008).
[30] Y. H. Shih, Front. Phys. China **2**, 125 (2007).
[31] J. H. Shapiro, Phys. Rev. A **78**, 061802(R) (2008).
[32] L. H. Ou and L. M. Kuang, J. Phys. B **40**, 1833 (2007).
[33] Y. F. Bai and S. S. Han, Phys. Rev. A **76**, 043828 (2007).
[34] J. B. Liu and Y. H. Shih, Phys. Rev. A **79**, 023819 (2009).
[35] D. Z. Cao, J. Xiong, S. H. Zhang, L. F. Lin, L. Gao, and K. G. Wang, Appl. Phys. Lett. **92**, 201102 (2008).
[36] I. N. Agafonov, M. V. Chekhova, T. Sh. Iskhakov, and A. N. Penin, J. Mod. Opt. **56**, 422 (2009).
[37] X. H. Chen, I. N. Agafonov, K. H. Luo, Q. Liu, R. Xian, M. V. Chekhova, and L. A. Wu, e-print arXiv:0902.3713; Opt. Lett. **35**, 1166 (2010).
[38] K. W. C. Chan, M. N. O'Sullivan, and R. W. Boyd, Opt. Lett. **34**, 3343 (2009).
[39] I. N. Agafonov, M. V. Chekhova, T. Sh. Iskhakov, and A. N. Penin, Phys. Rev. A **77**, 053801 (2008).
[40] Th. Richter, Phys. Rev. A **42**, 1817 (1990).
[41] L. Mandel and L. Wolf, *Optical Coherence and Quantum Optics* (Cambridge University Press, Cambridge, 1995), p. 428.
[42] D. Z. Cao, J. Xiong, and K. G. Wang, Phys. Rev. A **71**, 013801 (2005); D. Z. Cao and K. G. Wang, Phys. Lett. A **333**, 23 (2004).
[43] Y. T. Zhang, C. J. He, H. G. Li, and K. G. Wang, Chin. Phys. Lett. **25**, 2481 (2008).
[44] M. Bache, D. Magatti, F. Ferri, A. Gatti, E. Brambilla, and L. A. Lugiato, Phys. Rev. A **73**, 053802 (2006).